

## COMMUNICATION

# Atmospherically relevant core-shell aerosol studied using optical trapping and Mie scattering

Cite this: DOI: 10.1039/x0xx00000x

S. H. Jones,<sup>a,b</sup> M. D. King<sup>b</sup> and A. D. Ward<sup>\*a</sup>

Received 00th January 2012,

Accepted 00th January 2012

DOI: 10.1039/x0xx00000x

[www.rsc.org/](http://www.rsc.org/)

**Solid core-liquid shell aerosol have been trapped in a counter-propagating optical trap confirming potential core-shell morphology in the atmosphere. Mie spectroscopy can be used to measure the core radius and film thickness to 0.5 and 1 nm precision and measure the wavelength dependent refractive indices of silica (core) and oleic acid (shell).**

Atmospherically relevant core-shell aerosol has been generated and studied in the laboratory with precise ( $\pm 1$  nm) determination of shell thickness. The combination of optical trapping and Mie scattering has been used to study oleic acid coated silica beads and to determine the core silica size to  $\pm 0.5$  nm and the wavelength dependent refractive index to an uncertainty of  $\sim 0.0008$  at 589 nm. Oleic acid shell thickness has been determined to  $\pm 1$  nm and the wavelength dependent refractive index of the shell can be described by an uncertainty of  $\sim 0.0007$  at 589 nm.

The prevalence of aerosols in the lowest layer of the atmosphere, the troposphere, is well known<sup>1</sup>, however, their contribution to the Earth's climate remains uncertain<sup>1</sup>. Aerosols contribute to the climate in two ways; directly by scattering and absorbing solar radiation, and indirectly, by acting as cloud condensation nuclei (CCN) and influencing cloud radiative properties<sup>1</sup>. Aerosols exist as a complex mixture of chemicals<sup>2</sup> and morphologies, which influences their ability to form CCN and scatter or absorb radiation. Organic coatings are thought to exist on the surface of aerosols<sup>3-11</sup> but direct evidence is difficult to obtain as atmospheric sampling and subsequent analytical techniques such as Electron Microscopy (EM) often require contact methods which can change the morphology of the sampled aerosol. The presence of an organic coating or shell surrounding the aerosol core has the ability to influence water uptake of an aerosol<sup>11</sup>, the amount of scattered light<sup>12</sup> or absorbed solar radiation and to affect how the aerosol behaves in subsequent heterogeneous reaction with gas-phase oxidants. It is therefore important to

characterise the optical properties of coated aerosols to further understand their effect on the climate.

Mineral dust aerosol is one of the most prevalent sources of solid atmospheric aerosol, it is emitted into the atmosphere at around 1000-4000 Tg per year<sup>1</sup>. Typical mineral particle diameters range from 0.5  $\mu\text{m}$  to 100  $\mu\text{m}$  and contain silica<sup>13</sup>. Silica beads of approximately 1  $\mu\text{m}$  radius were therefore selected to represent solid aerosol. Once airborne, mineral aerosol may come into contact with a large variety of chemical species and can become coated. Oleic acid is a typical organic component found in the troposphere<sup>14</sup>, and was selected as the coating material for the silica beads in this experiment. The study reported here details the use of a counter-propagating optical trap and Mie scattering to study and characterise laboratory generated aerosol of silica beads coated with oleic acid.

There have been a number of contact and non-contact studies on core-shell systems reported in the literature, e.g.<sup>15-27</sup>. The most relevant study is that by Hightower et al.<sup>18</sup>, who trapped glass microspheres of  $\sim 4$   $\mu\text{m}$  radius in vacuum using a quadrupole trap. The glass beads were coated in glycerine and the scattered light intensity was recorded at a fixed angle during the evaporation of glycerine. Changes in intensity were compared to calculations based on Mie theory to confirm that a concentric layered sphere was trapped. Other associated core-shell studies<sup>22,23</sup> have also been conducted on chemicals not commonly found in the atmosphere;  $\sim 20$   $\mu\text{m}$  radius Santovac 5 (polyphenol ether) droplets coated in a layer of Fomblin (perfluorinated polyether) levitated in an Electrodynamic balance (EDB).

In the current study we report, to the best of our knowledge, the first optical trapping study of an atmospherically relevant (in terms of composition, size and trapping medium) coated solid aerosol, characterised using white light Mie scattering. The wavelength dependent refractive indices of both the material that forms the coating and the core have been determined as well as the core

aerosol radius and coating thickness. We demonstrate that core-shell aerosol may form in the atmosphere.

A vertically aligned counter-propagating optical trap was used to trap individual silica beads (Bangs Laboratories, SS04N, Lot number 7920, non-porous, 1.035  $\mu\text{m}$  radius) in dry nitrogen (relative humidity < 10 %) as a proxy for mineral dust. The optical trapping of silica beads has been studied in detail by Rkiouak et al<sup>28</sup>. Of the 35 silica beads captured in our study, the surface of 17 beads were coated with a thin film of oleic acid. Three of these coated beads were selected, at random, for detailed characterisation and analysis. The optical set-up has been described in detail in a previous publication<sup>29</sup> and will only be briefly discussed here. Once trapped, the aerosol is illuminated with white light from an LED, and the backscattered light from the particle is collected and directed into a spectrograph to produce a Mie spectrum as shown in Figure 1.

To use core-shell Mie theory for determining the oleic acid shell thickness the dispersion of refractive index of silica particles and oleic acid droplets were measured separately and these values were then applied to the core-shell Mie calculation without further change. Silica is optically well characterised; however, the refractive index of a silica bead can vary depending on the method of manufacture, specifically at the surface of the bead. Values of refractive index for oleic acid at the sodium D line are widely available in the literature<sup>30</sup> but the wavelength dependent dispersion is not well reported.

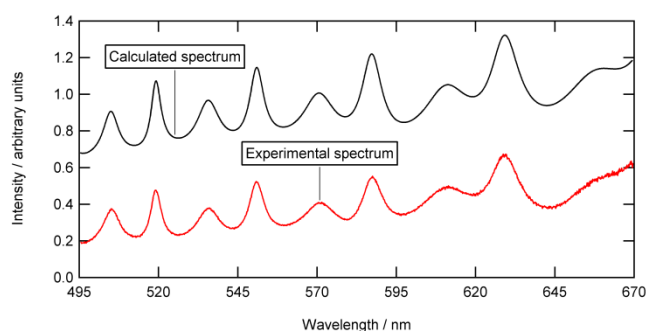


**Fig.1** A typical experimental Mie spectrum is shown in the lower trace (red) for an optically trapped oleic acid droplet. The upper trace (black) is the calculated Mie theory model for a trapped droplet of radius 1.0551  $\mu\text{m}$ , having a refractive index dispersion of,  $n = 1.4554 + \frac{4565}{\lambda^2} + \frac{1 \times 10^8}{\lambda^4}$ .

To determine the refractive index dispersion of oleic acid, a 0.1  $\text{g L}^{-1}$  solution of sodium chloride was atomised and dried to produce Aitken nuclei in nitrogen which were passed over a heated oleic acid reservoir held at a temperature of between 120-130°C. The flow was then cooled to produce oleic acid droplets that were carried in nitrogen into the trapping cell. An oleic acid droplet was trapped and grown in size through collisions with other oleic acid droplets until it was  $\sim 2 \mu\text{m}$  in diameter. A typical Mie spectrum for the resulting trapped droplet of oleic acid is shown in Figure 1. Mie theory<sup>31</sup> was used to model the measured Mie spectrum and determine the droplet radius and the wavelength dependent refractive index of oleic acid. The dispersion relation was found by numerically determining the global minimum in deviation between experimental data and the calculated Mie theory spectrum when

varying size and refractive index dispersion<sup>29</sup>. The error in identifying the position of the global minimum was propagated to the reported errors in particle size and refractive index. There is an excellent agreement between the calculated and experimental Mie spectrum, as evidenced by the root mean square value of  $\chi = 0.1764 \text{ nm}$ , (the average difference in wavelength per peak between the calculated and experimental peak positions<sup>29</sup>) and the traces in Figure 1. The determination of the wavelength dependent dispersion for the oleic acid is specific to our experimental conditions and, as such, is ideally suited for application to the core-shell model rather than using a literature value reported at a single wavelength.

Following the determination of the wavelength dependent dispersion of an oleic acid droplet, the next step was to trap a silica bead and characterise its size and wavelength dependent refractive index. The trapping cell was cleaned and dried and silica beads were atomised and carried to the cell in nitrogen. A single silica bead was optically trapped in air and illuminated with white LED light, resulting in a Mie spectrum, as shown in Figure 2. Mie theory was then used to model the experimental data. The determined refractive index for the silica bead shown in Figure 2 is 1.3664 at 589 nm which is in agreement with other studies<sup>32,33</sup> (1.3732 and 1.3933) conducted on silica beads from the same manufacturer.

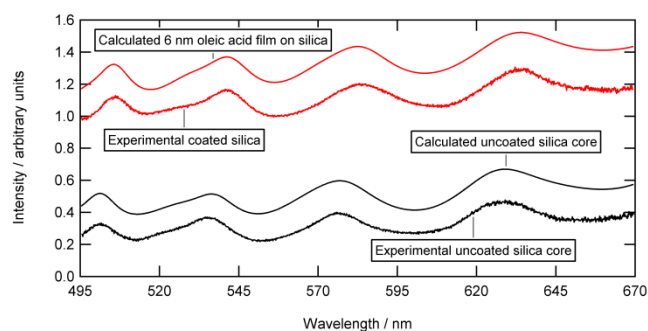


**Fig.2** The lower two traces (black) show a typical experimental Mie spectrum for an optically trapped silica bead (lowest trace) and its Mie model (trace above) for a silica bead of 0.9559  $\mu\text{m}$  radius, with a refractive index dispersion of,  $n = 1.3548 + \frac{3720}{\lambda^2} + \frac{1 \times 10^8}{\lambda^4}$ . The upper two traces (red) represent a coated experimental Mie spectrum (lower trace) after 140 seconds exposure to oleic acid vapour and the core-shell Mie model (uppermost trace) for a 6 nm thick oleic acid film on the core silica bead.

**Table 1** Radii and refractive index dispersions for an oleic acid droplet and three individual silica beads obtained using Mie theory<sup>31</sup>

Species	Radius / $\mu\text{m}$	A	B / $\text{nm}^2$	C / $\text{nm}^4$	$\chi$ / nm
Oleic acid	1.0551 $\pm$ 0.0004	1.4554 $\pm$ 0.0005	4565 $\pm$ 70	$1 \times 10^8$	0.1764
Silica 1	0.957 $\pm$ 0.0005	1.3587 $\pm$ 0.0007	3250 $\pm$ 100	$1 \times 10^8$	0.3715
Silica 2	0.9493 $\pm$ 0.0005	1.3609 $\pm$ 0.001	2995 $\pm$ 35	$1 \times 10^8$	0.3729
Silica 3	0.9559 $\pm$ 0.0005	1.3548 $\pm$ 0.001	3720 $\pm$ 50	$1 \times 10^8$	0.3136

<sup>a</sup> Footnote text.

Following determination of the parameters in Table 1, the trapped silica beads were coated with oleic acid by producing a supersaturation of oleic acid vapour in the trapping environment. A

flow of nitrogen was passed over a heated oleic acid reservoir (between 110–130°C) and subsequently cooled to room temperature and directed into the trapping cell, where the oleic acid condensed on to the surface of the silica bead to form a uniform thin film. Mie spectra were recorded throughout the coating process to assess film formation and measure film thickness.

On exposure to a supersaturated environment of gaseous oleic acid the position of the Mie peaks shifted to longer wavelengths in comparison to that of uncoated silica, which was indicative of thin film formation. An example spectrum illustrating this shift is shown in Figure 2 for a 6 nm oleic acid film. The experimental shifts for each peak in the spectrum throughout the coating process can be seen in Figure 3. With increasing exposure time to gaseous oleic acid, the experimental peak positions shifted to longer wavelengths, indicative of an increase in film thickness. Core-shell Mie theory<sup>34,35</sup> was used to determine the film thickness at selected time points throughout the experiment and is highlighted in Figure 3. The film thickness increases with prolonged exposure time to oleic acid and the measured film thickness increases from 3 nm to 11 nm ± 1 nm for the selected time points in Figure 3. Previous studies on larger particles have observed a poorer quality of fit with increasing film thickness for thicker films<sup>17,20</sup>. Kaiser et al.<sup>20</sup>, stated the different densities of the coating and core material could influence formation of a non-concentric coating.

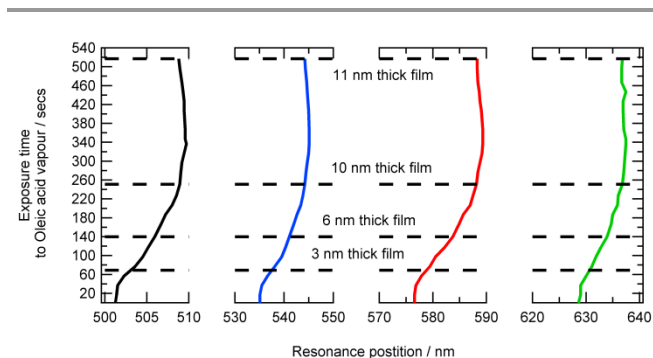


**Fig. 3** The solid lines show the four peak positions shifting with increasing exposure time to gaseous oleic acid for Silica bead 3 in Table 1. The dashed lines indicate where experimental peaks shifts correspond to the stated oleic acid film thicknesses calculated from core-shell Mie theory<sup>34,35</sup>.

From the agreement between experimental and calculated data for a core-shell system we conclude that the silica bead is uniformly coated. If the bead were non-uniformly coated, e.g. if a 'droplet' of coating material was present on one part of the silica surface, there would be a reduction in intensity of the experimental positions. Depending on the exact geometry of the system, it could also be possible to observe almost a complete disappearance of the Mie spectrum<sup>36</sup>. Neither of these effects was observed experimentally.

Other effects were also considered, such as, laser heating, a change in the refractive index of the surrounding medium, or loss of symmetry in aerosol morphology. Laser heating from 25 mW of laser trapping power could cause a temperature increase in the trapped uncoated silica bead. Assuming a conservative 1°C temperature increase<sup>37</sup>, the associated thermal expansion of the silica bead would cause the peak positions to shift wavelength by < 1 nm, which is negligible when compared to the peak shifts arising from the

presence of a 1 nm oleic acid film on a trapped silica bead > 1 nm. Peak shifts arising from changes in the refractive index of the surrounding medium i.e. the difference of a bead being trapped in dry or moist air result in peak shifts of < 1 nm. It is also assumed that the trapped particle is spherical, as we do not observe splitting or broadening of the Mie peaks<sup>38,39</sup>.

From the detailed analysis of three experimental spectra, the agreement between our calculated results using core-shell Mie theory<sup>34,35</sup> and our experimental data indicates that we have successfully formed a concentric coating of oleic acid on an optically trapped silica bead. The coating is also seen to increase in thickness with increasing exposure time to a supersaturated vapour of oleic acid. It is likely that this geometry will exist naturally if it formed in the laboratory from atmospheric proxies of silica and oleic acid and therefore could be influential in the atmosphere.

The ability to generate core-shell aerosol and assess shell growth combined with the determination of the wavelength dependent refractive index of both the core aerosol and the shell indicates an important step in atmospheric chemistry, towards further understanding the impact of coated aerosol on the atmosphere. Further studies into different core-shell systems and heterogeneous reactions are required to verify the hypothesis.

The authors would like to thank the Central Laser Facility for laboratory access at the Research Complex at Harwell under grants 13230007, 12230019 and 12130016. SHJ would like to acknowledge NERC for PhD funding grant NE/HC1903/1.

## Notes and references

<sup>a</sup> Central Laser Facility, Research Complex at Harwell, Rutherford Appleton Laboratory, Didcot, Oxon, OX11 0FA, UK. E-mail: andy.ward@stfc.ac.uk

<sup>b</sup> Department of Earth Sciences, Royal Holloway, University of London, Egham, Surrey, TW20 0EX, UK.

† Footnotes should appear here. These might include comments relevant to but not central to the matter under discussion, limited experimental and spectral data, and crystallographic data.

Electronic Supplementary Information (ESI) available: [details of any supplementary information available should be included here]. See DOI: 10.1039/c000000x/

- 1 Climate Change 2013: The Physical Science Basis. Working Group I Contribution to the Fifth Assessment Report of the Intergovernmental Panel on Climate Change, Cambridge University Press, Cambridge, United Kingdom, 2014.
- 2 U. Pöschl, *Angew. Chem. Int. Ed. Engl.*, 2005, **44**, 7520–7540.
- 3 D. C. Blanchard, *Science*, 1964, **146**, 396–397.
- 4 G. B. Ellison, F. Tuck, and V. Vaida, 1999, **104**, 11633–11641.
- 5 D. J. Donaldson and V. Vaida, *Chem. Rev.*, 2006, **106**, 1445–1461.
- 6 P. S. Gill, T. E. Gradel, and C. J. Weschler, *Rev. Geophys. Sp. Phys.*, 1983, **21**, 903–920.
- 7 H. Tervahattu, K. Hartonen, V. Kerminen, K. Kupiainen, T. Koskentalo, A. F. Tuck, and V. Vaida, *J. Geophys. Res.*, 2002, **107**.
- 8 B. E. Wyslouzil, G. Wilemski, R. Strey, C. H. Heath, and U. Dieregswiler, *Phys. Chem. Chem. Phys.*, 2006, **8**, 54–57.
- 9 A. H. Falkovich, *J. Geophys. Res.*, 2004, **109**, D02208.
- 10 D. M. Cwiertny, M. A. Young, and V. H. Grassian, *Annu. Rev. Phys. Chem.*, 2008, **59**, 27–51.

- 11 M. D. King, K. C. Thompson, and A. D. Ward, *J. Am. Chem. Soc.*, 2004, **126**, 16710–16711.
- 12 Y. Li, M. J. Ezell, and B. J. Finlayson-pitts, *Atmos. Environ.*, 2011, **45**, 4123–4132.
- 13 K. H. Wedepohl, *Geochim. Cosmochim. Acta*, 1995, **59**, 1217–1232.
- 14 W. F. Rogge, L. Hildemann, M. A. Mazurek, G. R. Cass, and B. Simoneit, *Environ. Sci. Technol.*, 1991, **25**, 1112–1125.
- 15 E. R. Garland, A. D. Lee, T. Baer, and L. I. Clarke, *J. Phys. Chem. C*, 2009, **113**, 2141–2148.
- 16 Y. Katrib, S. Martin, H. Hung, Y. Rudich, H. Zhang, J. G. Slowik, P. Davidovits, J. T. Jayne, and D. R. Worsnop, *J. Phys. Chem. A*, 2004, **108**, 6686–6695.
- 17 A. Abo Rizeq, M. Trainic, C. Erlick, E. Segre, and Y. Rudich, *Atmos. Chem. Phys.*, 2008, **8**, 1823–1833.
- 18 R. L. Hightower, C. B. Richardson, H. B. Lin, J. D. Eversole, and A. J. Campillo, *Opt. Lett.*, 1988, **13**, 946–948.
- 19 W. Li, S. Rassat, W. Foss, and E. Davis, *J. Colloid Interface Sci.*, 1994, **162**, 267–278.
- 20 T. Kaiser, G. Roll, and G. Schweiger, *Appl. Opt.*, 1996, **35**, 5918–5924.
- 21 J. F. Widmann, C. L. Aardahl, T. J. Johnson, and E. J. Davis, *J. Colloid Interface Sci.*, 1998, **199**, 197–205.
- 22 J. Huckaby and A. Ray, *Langmuir*, 1995, **11**, 80–86.
- 23 A. K. Ray and R. Nandakumar, *Appl. Opt.*, 1995, **34**, 7759–7770.
- 24 D. P. Veghte, M. B. Altaf, and M. A. Freedman, *J. Am. Chem. Soc.*, 2013, **135**, 16046–16049.
- 25 J. Buajarern, L. Mitchem, and J. P. Reid, *J. Phys. Chem. A*, 2007, **111**, 9054–9061.
- 26 B. J. Dennis-Smith, K. L. Hanford, N.-O. A. Kwamena, R. E. H. Miles, and J. P. Reid, *J. Phys. Chem. A*, 2012, **116**, 6159–6168.
- 27 M. Song, C. Marcolli, U. K. Krieger, D. M. Lienhard, and T. Peter, *Faraday Discuss.*, 2013, **165**, 289–316.
- 28 L. Rkiouak, M. J. Tang, J. C. J. Camp, J. McGregor, I. M. Watson, R. A. Cox, M. Kalberer, A. D. Ward, and F. D. Pope, *Phys. Chem. Chem. Phys.*, 2014, **16**, 11426–11434.
- 29 S. H. Jones, M. D. King, and A. D. Ward, *Phys. Chem. Chem. Phys.*, 2013, **15**, 20735–20741.
- 30 CRC Handbook of Chemistry and Physics, CRC Press, Taylor and Francis, Boca Raton, FL, 86th edition, 3-406 and 10-249, 2005.
- 31 C. F. Bohren, D. R. Huffman, *Absorption and Scattering of Light by Small Particles*, Wiley, 1998.
- 32 J. J. Valle-Delgado, J. A. Molina-Bolívar, F. Galisteo-González, M. J. Gálvez-Ruiz, a Feiler, and M. W. Rutland, *J. Chem. Phys.*, 2005, **123**, 34708.
- 33 R. S. Conroy, B. T. Mayers, D. V. Vezenov, D. B. Wolfe, M. G. Prentiss, and G. M. Whitesides, *Appl. Opt.*, 2005, **44**, 7853–7857.
- 34 A. L. Aden and M. Kerker, *J. Appl. Phys.*, 1951, **22**, 1242–1246.
- 35 O. B. Toon and T. P. Ackerman, *Appl. Opt.*, 1981, **20**, 3657–3660.
- 36 J. P. Reid, B. J. Dennis-Smith, N.-O. A. Kwamena, R. E. H. Miles, K. L. Hanford, and C. J. Homer, *Phys. Chem. Chem. Phys.*, 2011, **13**, 15559–15572.
- 37 R. J. Hopkins, L. Mitchem, A. D. Ward, and J. P. Reid, *Phys. Chem. Chem. Phys.*, 2004, **6**, 4924–4927.
- 38 S. Arnold, D. E. Spock, and L. M. Folan, *Opt. Lett.*, 1990, **15**, 1111–1113.
- 39 G. Schweiger, *Opt. Lett.*, 1990, **15**, 156–158.